

Density Profile of Cool Core of Galaxy Clusters

Naomi OTA,¹ Kiyokazu ONZUKA,² and Kuniaki MASAI²

¹*Department of Physics, Nara Women's University, Kita-uoyanishi-machi, Nara 630-8506*
naomi@cc.nara-wu.ac.jp

²*Department of Physics, Tokyo Metropolitan University, 1-1 Minami-Osawa, Hachioji, Tokyo 192-0397*

(Received ; accepted)

Abstract

The density profile of cool core of intracluster gas is investigated, for a cluster of galaxies that is initially in the virial equilibrium state and then undergoes radiative cooling. The initial gas profile is derived under the assumption that the gas is hydrostatic within the dark matter potential presented by so-called NFW or King model and has a polytropic profile. The contribution from masses of gas and galaxies to the potential is ignored compared to the dark matter in the calculation. The temperature and density profiles of gas in its quasi-hydrostatic cooling phase, which is expected to last for \sim Gyr, is then calculated for different initial gas profiles. It is found that in the quasi-hydrostatic cooling phase, while the temperature decreases to be about one-third, the density increases by a factor of 4–6 at the cluster center in comparison with their initial polytropic values, though the profiles over the core depend on the dark matter potential. Hence, the core radius in the quasi hydrostatic cooling gas appears smaller than the initial polytropic one. We compare the density profile of the cool core with observations to find that while the initial density is around the upper bounds of large-core (> 100 kpc) clusters, likely most relaxed but cooling is not yet significant, the central density under quasi-hydrostatic cooling falls between the mid- and high-values of small-core (< 100 kpc) or cool-core clusters. It is also found for the quasi-hydrostatic cooling gas that the entropy profile roughly agrees with the best-fit model for the ACCEPT cluster sample with a low central entropy, and the pressure gradient in the inner core is close to that of the REXCESS sample. X-ray surface brightness calculated for the quasi-hydrostatic cooling gas is well represented by the conventional double β -model, giving a physical basis of applying the double β -model to cool core clusters.

Key words: galaxies: clusters: general – cooling flows – galaxies: intergalactic medium – X-rays: galaxies: clusters

1. Introduction

Clusters of galaxies offer excellent laboratories for thermal evolution of cosmic baryons: the objects are filled with hot ($T \sim 10^7 - 10^8$ K), highly-ionized intracluster gas and the baryon fraction in massive clusters is close to the cosmic value. Since the timescale of radiative cooling at the center of regular clusters is estimated to be shorter than the Hubble time, their core regions are thought to be affected by cooling. According to statistical studies of clusters using X-ray observations, the fraction of clusters having a compact, cool core (often termed CC clusters), is roughly 50% (e.g., O'Hara et al. 2006; Ota et al. 2006; Chen et al. 2007; Santos et al. 2008; Cavagnolo et al. 2009; Hudson et al. 2010).

Based on earlier works on peaked surface-brightness that cooling core clusters exhibit, it was suggested that global cooling-flow would occur unless some heating process balances with radiative cooling (e.g., Fabian 1994). The similarity and smoothness of cooling profiles indicate need for continuous, distributed heat source (for review, e.g., Peterson & Fabian 2006). On the other hand, a possible mild inflow with a quasi-hydrostatic balance is proposed to account for observed temperature profiles of cooling cores (Masai & Kitayama 2004). Later, using

a hydrodynamics code, Akahori & Masai (2006) demonstrate that such a cooling phase lasts for \sim Gyr and then breaks into the global cooling-flow. They discuss the origin of observed two-peaked core size distribution (Ota & Mitsuda 2002; Ota & Mitsuda 2004) in view of the thermal evolution.

While intracluster gas has often been studied on the basis of the conventional isothermal β -model, a deviation therefrom has been commonly observed at the center of cool core clusters: they exhibit a systematically higher central density while the profiles are fairly universal outside $0.1r_{500} \sim 100$ kpc (e.g., Neumann & Arnaud 1999). To better reproduce those X-ray observations, some authors have introduced empirical models such as double- β model (e.g., Jones & Forman 1984) and modified β model with a cool density cusp at the center and steepening at a large radius (Vikhlinin et al. 2006). This model gave a good fit to the high-resolution *Chandra* data including the core emission (see also Bulbul et al. 2010). Although those models are given in analytic forms and therefore simply utilized for observational studies, physical background that they are based on is not always clear.

In the present paper, we intend to obtain a fiducial density profile of cooling gas under quasi-hydrostatic balance. Masai & Kitayama (2004) give a temperature profile for

the *initially* isothermal gas, but no density one. We calculate the temperature of cooling gas in the same manner but consider more generally that the gas is initially hydrostatic with an polytropic profile in the NFW (Navarro et al. 1997) or King dark matter potential. In section 2, our model calculation is described, and pressure and entropy as well as density of quasi-hydrostatic cooling gas are presented. In section 3, we compare those calculated quantities with observations, and also examine application of widely used β -model to X-ray surface brightness calculated for quasi-hydrostatic cooling gas. We then discuss implications on the ICM thermal evolution in the cluster core regions. Since the profiles of gas density etc. of cool cores are of our interest, we present the quantities normalized to their central values unless specified otherwise.

2. Calculations

2.1. Initial hydrostatic gas distribution

We consider a spherically symmetric galaxy cluster initially in the virial equilibrium. We ignore the mass of the gas and galaxies compared to the dark matter, which is thought to occupy typically more than 80% of the cluster mass. Thus, the gas distributes so that its pressure balances with the local gravitational potential formed by the dark matter. For non-cool core (NCC), i.e, for the initial state before cooling becomes significant, we assume that the gas is in a hydrostatic balance,

$$\frac{1}{\rho} \frac{dP}{dr} = -\frac{d\phi}{dr} \simeq -G \frac{M_{\text{DM}}(r)}{r^2}, \quad (1)$$

where P and ρ are the gas pressure and density, respectively, and ϕ the gravitational potential and $M_{\text{DM}}(r)$ is the dark matter mass contained in a radius r . We solve equation (1) with an equation of state as $P \propto \rho^\gamma$ to obtain the initial gas distribution, where $\gamma = 1 + 1/N$ for the polytrope index N . We consider the NFW distribution and approximated King distribution (referred to as King distribution hereafter) for the dark matter potential as shown in figure 1.

The gas temperature profile thus obtained for the NFW potential can be expressed in a form

$$\frac{T(r^*)}{T(0)} = 1 - \frac{\gamma - 1}{\gamma} \frac{U_G}{kT(0)} \left[1 - \frac{\log(1 + r^*)}{r^*} \right] \quad (2)$$

with

$$r^* = \frac{r}{r_s} \quad \text{and} \quad U_G = \frac{\mu m G}{r_s} 4\pi r_s^3 \delta_c \rho_c, \quad (3)$$

where r_s is the characteristic radius of the NFW distributions expressed as

$$\rho_{\text{DM}}(r^*) = \frac{\delta_c \rho_c}{r^*(1 + r^*)^2}, \quad (4)$$

and $\delta_c \rho_c$ is a constant related with the dark matter mass M_{DM} through

$$M_{\text{DM}}(r^*) = 4\pi r_s^3 \delta_c \rho_c \left[\log(1 + r^*) + \frac{1}{1 + r^*} - 1 \right]. \quad (5)$$

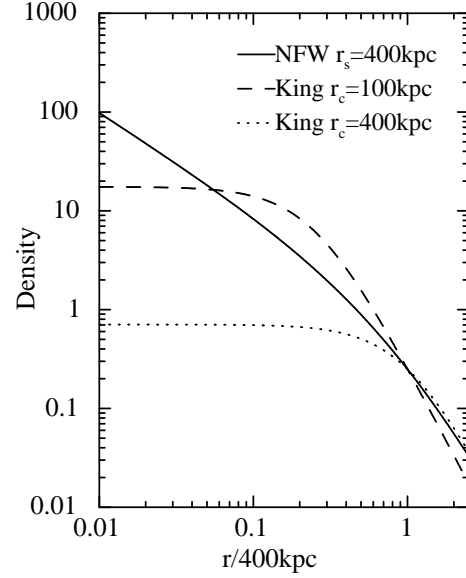


Fig. 1. Dark matter density profiles with $r_s = 400$ kpc for the NFW (solid) and $r_c = 100$ kpc for the King (broken) distribution taken into calculations here (see text). The King profile with $r_c = 400$ kpc is also shown for reference. The three curves are normalized so as to pass the same point at $r = 400$ kpc.

The gas density profile is given by

$$\frac{\rho(r^*)}{\rho(0)} = \left[\frac{T(r^*)}{T(0)} \right]^{1/(\gamma-1)} = \left[\frac{T(r^*)}{T(0)} \right]^n. \quad (6)$$

For the King potential, similarly we obtain the gas temperature as

$$\frac{T(r^*)}{T(0)} = 1 - \frac{\gamma - 1}{\gamma} \frac{U_G}{kT(0)} \left[1 - \frac{\log(r^* + \sqrt{r^{*2} + 1})}{r^*} \right] \quad (7)$$

with

$$r^* = \frac{r}{r_c} \quad \text{and} \quad U_G = \frac{\mu m G}{r_c} 4\pi r_c^3 \rho_0. \quad (8)$$

Here r_c is the core radius of the King distribution expressed as

$$\rho_{\text{DM}}(r^*) = \frac{\rho_0}{(1 + r^{*2})^{3/2}}, \quad (9)$$

where ρ_0 is the dark matter density at the center. The dark matter mass is given by

$$M_{\text{DM}}(r^*) = 4\pi r_c^3 \rho_0 \left[\log(r^* + \sqrt{r^{*2} + 1}) - \frac{r^*}{\sqrt{r^{*2} + 1}} \right]. \quad (10)$$

The gas density profile for the King potential is given by equation (6) as well.

The density profiles, $\rho(r)/\rho(0)$, calculated from the above equations are shown by the broken lines (denoted by NCC) in figure 2 with $r_s = 400$ kpc for the NFW and $r_c = 100$ kpc for the King dark matter potentials. These radii are chosen for the β -model core radius of surface brightness ($\propto \rho^2 T^{1/2}$) to give nearly the same radii of 100–200 kpc as each other. The equations (2)–(6) are

equivalent to those (12) and (42)–(46) in Suto, Sasaki & Makino (1998), and therefore the broken lines in the *left* panel (NFW NCC) of figure 2 are the same results as theirs. We calculate the temperature profile, $T(r)/T(0)$, as well for calculations in the following section.

2.2. Quasi-hydrostatic gas distribution under radiative cooling

Now we consider gas distribution of a cool core (CC) that significantly undergoes radiative cooling. The gas is then no longer in the hydrostatic balance but should be described by hydrodynamics, since inflow toward the inner region where the cooling rate is higher would occur so as to compensate the pressure decrease due to radiation loss (Fabian 1994). Hence, the gas temperature and density profiles of the cluster core deviate from those polytropic profiles given in the last subsection.

In the early cooling phase, however, inflow is yet mild and quasi-hydrostatic condition is attained marginally until the initial cooling time τ_{cool} . Here τ_{cool} is defined with the density and temperature at the center of a virialized cluster before cooling and is typically $\sim \text{Gyr}$ (Akahori & Masai 2006). We consider that the pressure decrease at a radius due to radiation is compensated immediately by gas inflow from the adjacent outer (and hotter) region, or the local inflow rate is controlled by the local cooling rate, and thus quasi-hydrostatic condition is attained.

The profile of the cooling gas temperature, $T'(r)$, is then expressed approximately in a form (Masai & Kitayama 2004)

$$\frac{d \ln T'}{d \ln r} \simeq \frac{9}{5} \left(1 - \frac{1}{3} \beta_T \frac{T_0}{T'} \right) \quad (11)$$

at $0 < r \leq r_{\text{cool}}$, when variation of $T(r)$ (NCC) is enough small in this range; it should be noted that this equation was obtained originally for isothermal mass distribution of the virial temperature T_0 . Here, r_{cool} is a cooling core radius in which the local cooling time is shorter than the Hubble time, as $t_{\text{cool}}(r) = 3kT(r)/[2\rho(r)\Lambda] < H_0^{-1}$ at $r < r_{\text{cool}}$ and $t_{\text{cool}}(r_{\text{cool}}) = H_0^{-1}$, where $\rho\Lambda$ represents the radiative cooling rate per unit time. We assume $\beta_T = 1$, i.e., the gas and dark matter have the same temperatures as each other. In observations, the values of β implied by the density profile fall around 0.6 less than unity. This may, however, be a result inherent to the β -model because it is normally applied to observed profiles within a radius significantly smaller than the viral radius (see Akahori & Masai 2005). We put $T(0) = T_0$ for normalization and calculate $T'(r)/T(0)$ with a boundary condition $T'(r_{\text{cool}}) = T(r_{\text{cool}})$. It should be noted that $T(r_{\text{cool}})/T(0)$ depends on the potential profile and γ , and thus $T'(r)/T(0)$ does as well, though not explicitly seen in equation (11).

Once the gas inflow takes place to be steady and the quasi-hydrostatic condition is attained, we may have

$$\frac{1}{\rho'} \frac{dP'}{dr} \simeq \frac{1}{\rho} \frac{dP}{dr} \simeq -G \frac{M_{\text{DM}}(r)}{r^2}, \quad (12)$$

where ρ' and P' are the gas density and pressure, respec-

tively, of the cool core. The ram pressure is negligible compared to the thermal one in this balance. Thus, for given $T'(r)$ the density profile

$$\frac{d \ln \rho'}{d \ln r} \simeq -\frac{d \ln T'}{d \ln r} + \frac{T}{T'} \gamma \frac{d \ln \rho}{d \ln r} \quad (13)$$

follows; note that γ is defined for P (or T) and ρ . In the cool core concerned, T/T' varies with r from 1 at r_{cool} to ~ 3 at $r \sim 0$, and the gas is kept (quasi-) hydrostatic through the core. Actually, for inflow to occur, the left-hand side must be once larger than the right-hand side in equation (12); note that dP/dr is negative.

Using equation (13) with $T(r)$ and $\rho(r)$ obtained in the last section and $T'(r)$ from equation (11), we calculate $\rho'(r)/\rho(0)$ with $\rho'(r_{\text{cool}}) = \rho(r_{\text{cool}})$, and show in figure 2 by the solid lines (denoted by CC) for a typical cooling radius of $r_{\text{cool}} = 100$ kpc (e.g., Peterson & Fabian 2006). The initial gas density is taken to be a polytropic distribution of $\gamma = 1.001$ or 1.66 (see Section 2.1) and represented by the broken line (NCC). The virialized gas of $\gamma \simeq 1$ polytrope may be attained, e.g., if merger shocks are radiative or thermal conduction works through the core in the formation history of the cluster. Note that quasi-hydrostatic cooling (Masai & Kitayama 2004) predicts a steeper profile than the hydrostatic one of $\gamma = 1.001$ polytrope.

In figure 2, the dotted lines (denoted by β) represent the best-fit β -model, $n(r) = n_0 [1 + (r/r_{\text{c,gas}})^2]^{-3\beta/2}$ with n and $r_{\text{c,gas}}$ being the density and the core radius of gas, to mimic the density of CC at $5 < r/\text{kpc} < 100$. The parameters are given in table 1, where also is given the parameters for the initial non-cool cores in the range $5 < r/\text{kpc} < 400$. At $r < r_{\text{cool}}$ the β -model can reproduce the density of CC fairly well for the NFW and quite well for the King potential; systematically, the β -model gives a flat profile toward the center than calculated for the NFW. This result may suggest that analysis with the β -model is useful also for cool cores if the gas is quasi-hydrostatic, though not relevant to its original meaning.

Figure 3 shows the pressure profile, $\rho(r)T(r)/[\rho(0)T(0)]$ (broken lines, NCC) and $\rho'(r)T'(r)/[\rho(0)T(0)]$ (solid lines, CC). It is seen that in the quasi-hydrostatic cooling core ($r \lesssim r_{\text{cool}} = 100$ kpc) the pressure profile is steeper for the initially isothermal ($\gamma = 1.001$) gas than the $\gamma = 1.66$ gas, and for the NFW potential than the King one well inside r_{cool} . Also shown by the dotted line is the best-fit generalized NFW (GNFW, hereafter; Nagai et al. 2007) pressure obtained for the REXCESS sample of clusters (Arnaud et al. 2010 Eqs. 11–12), $p(x) = P_0[(c_{500}x)^{-\theta}(1 + (c_{500}x)^\zeta)]^{-(\eta-\theta)/\zeta}$ for $(P_0, c_{500}, \theta, \zeta, \eta) = (8.403h_{70}^{-3/2}, 1.177, 0.3081, 1.0510, 5.4905)$. The GNFW profile is normalized so as to pass the intersection of $\gamma = 1.001$ and $\gamma = 1.66$ curves of quasi-hydrostatic cooling gas (CC).

Figures 4 shows the entropy profile, $T(r)/\rho^{2/3}(r)/[T(0)/\rho(0)^{2/3}]$ (broken lines, NCC) and $T'(r)/\rho'^{2/3}(r)/[T(0)/\rho(0)^{2/3}]$ (solid lines, CC). While the initial polytropic gas (NCC) exhibits a flat or shallower profile, the cooling gas (CC) exhibits entropy roughly $\propto r$ at $0.1 < r/r_{\text{cool}} < 1$ for both the NFW and King

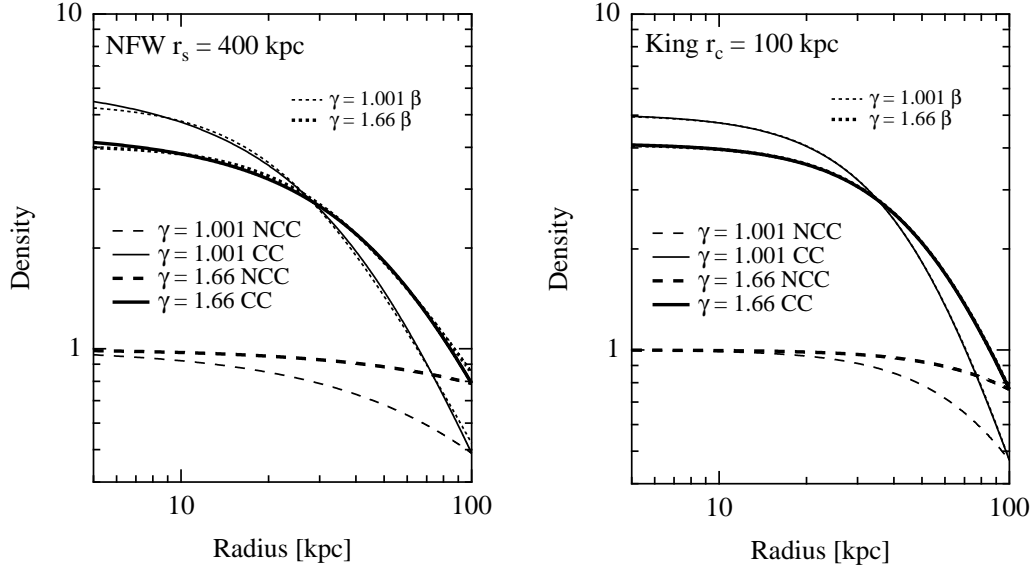


Fig. 2. Gas density profile of quasi-hydrostatic cool cores, $\rho'(r)/\rho(0)$ (solid lines, CC) with $r_{\text{cool}} = 100$ kpc and the initial non-cool ones, $\rho(r)/\rho(0)$ (broken lines, NCC) of $\gamma = 1.66$ (thick lines) or 1.001 (thin lines) polytrope. The dotted lines represent the best-fit β -model (see text). Particularly in the right panel, the best-fit β -models (thin and thick dotted lines) reproduce the calculated CC density profiles (thin and thick solid lines) well and almost perfectly overlap with them for both $\gamma = 1.001$ and 1.66 , respectively.

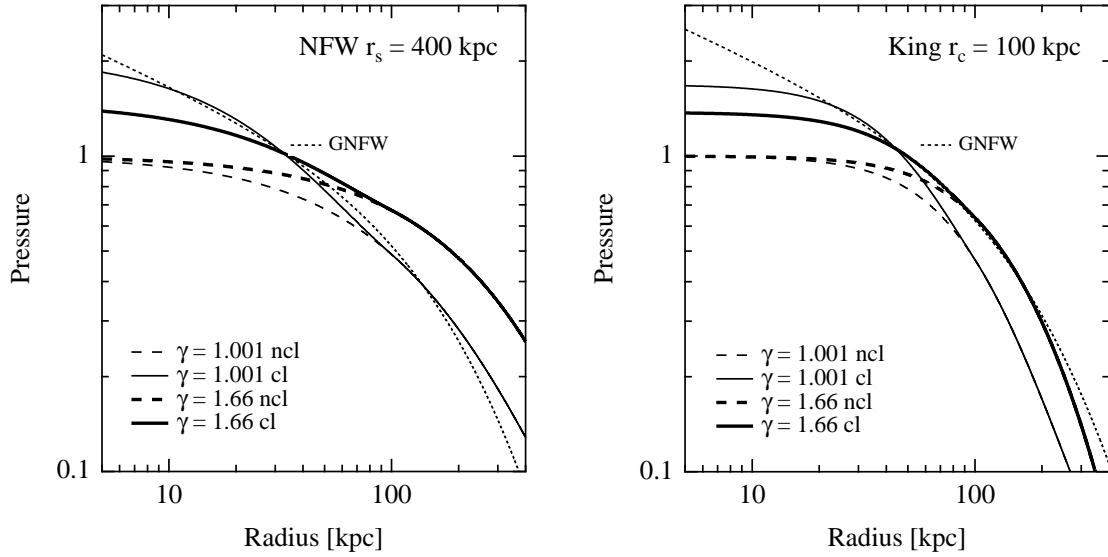


Fig. 3. Gas pressure profile of quasi-hydrostatic cool cores, $\rho'(r)T'(r)/[\rho(0)T(0)]$ (solid lines, CC) with $r_{\text{cool}} = 100$ kpc and the initial non-cool ones, $\rho(r)T(r)/[\rho(0)T(0)]$ (broken lines, NCC) of $\gamma = 1.66$ (thick lines) or 1.001 (thin lines) polytrope. The dotted lines represent the GFW pressure profile obtained for REXCESS sample by Arnaud et al. (2010) (see text).

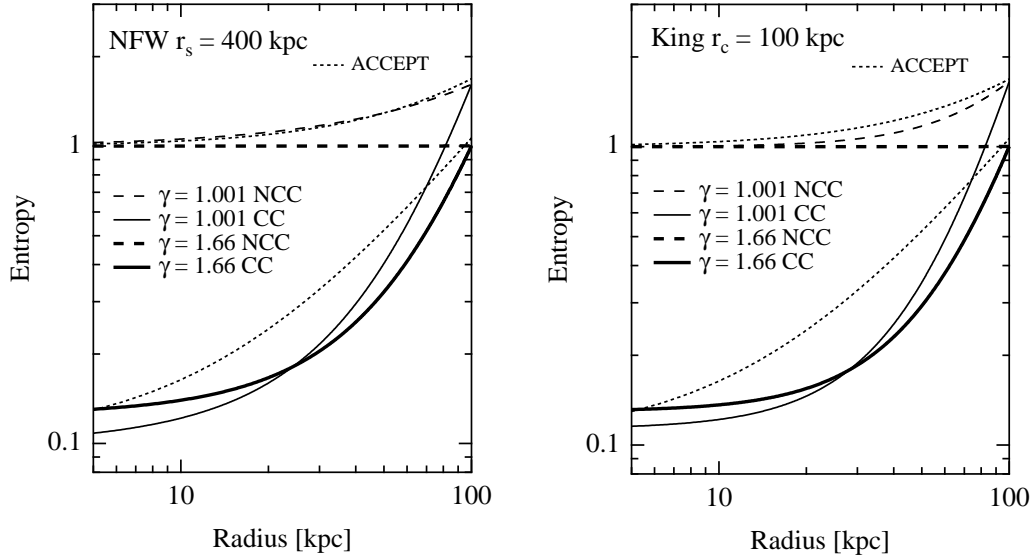


Fig. 4. Entropy profile of quasi-hydrostatic cool cores, $T'(r)/\rho^{2/3}(r)/[T(0)/\rho^{2/3}(0)]$ (solid lines, CC) with $r_{\text{cool}} = 100$ kpc and the initial non-cool ones, $T(r)/\rho^{2/3}(r)/[T(0)/\rho^{2/3}(0)]$ (broken lines, NCC) of $\gamma = 1.66$ (thick lines) or 1.001 (thin lines) polytrope. The upper and lower dotted curves in each panel indicate the best-fit entropy profiles for the ACCEPT sample with low ($K_0 \leq 50$ keV cm²) and high ($K_0 > 50$ keV cm²) central entropy values (Cavagnolo et al. 2009), respectively.

Table 1. β -model parameters for density profiles of non-cool and cool cores.

Potential		$\gamma = 1.001$			$\gamma = 1.66$		
		n_0^*	$r_{\text{c,gas}}$ [kpc]	β	n_0	$r_{\text{c,gas}}$ [kpc]	β
NFW	NCC	0.89 (1.00)	64	0.33	0.95 (1.00)	104	0.25
NFW	CC	5.41 (6.24)	25	0.55	4.05 (4.43)	33	0.45
King	NCC	1.00 (1.00)	100	0.53	0.99 (1.00)	164	0.44
King	CC	5.02 (5.05)	51	1.0	4.10 (4.13)	58	0.81

* Central density normalized to that for the non-cool core. The value in parenthesis denotes the central surface brightness obtained from the present calculation.

potentials. The best-fit profiles obtained by Cavagnolo et al. (2009) for the ACCEPT cluster sample are also shown with the dotted lines so as for their high central entropy K_0 (> 50 keV cm²) to be unity at $r = 0$. Note that their entropy profile consists of a power-law plus a constant, $K(r) = K_0 + K_{100}(r/100 \text{ kpc})^\alpha$, and the best-fit parameters are $(K_0, K_{100}, \alpha) = (16.1, 150, 1.20), (156, 107, 1.23)$ for clusters with $K_0 \leq 50$ and $K_0 > 50$ keV cm², respectively.

Comparison of the calculated density, pressure and entropy with observations is discussed in the next section. It should be noted here that r_{cool} is a point of discontinuity since we concern cooling within r_{cool} leaving the initial polytropic value as is outside.

The picture discussed in this section is valid as long as sound crossing time is enough shorter than τ_{cool} . In other words, without any heating process, sound speed decreases with cooling and eventually becomes unable to readjust pressure against the gravitational force. Flattening of $\rho'(r)$ toward the center is due to (quasi-) hydrostatic balance, and actual $\rho'(r)$ could be steeper in hydrodynamics. Note that T' or ρ' here is not applicable to the deep core where the gas accumulates, and also

recall that we ignore the gas mass for the gravitational potential. In the quasi-hydrostatic cooling phase, equation (12) or (13) can be a good approximation for typical cool cores. The results here are useful for β -model based or such hydrostatic balance based analysis, as discussed in the following section.

3. Discussion

3.1. Comparison with observed core radii and density profiles

As seen in figure 2 or table 1, the core radius in the quasi-hydrostatic cooling phase is about one-third of the initial radius of polytropic gas in the virial equilibrium. If clusters which are relaxed or virialized but not yet cooling-affected have ~ 200 kpc cores, the clusters in the quasi-hydrostatic cooling stage appear to be those of ~ 60 kpc cores. This result is consistent with the hydrodynamical calculations by Akahori & Masai (2006), who analyzed the calculated clusters with the β -model.

In figure 5, the gas density profiles are compared with the best-fit β -model profiles for clusters analyzed in Ota

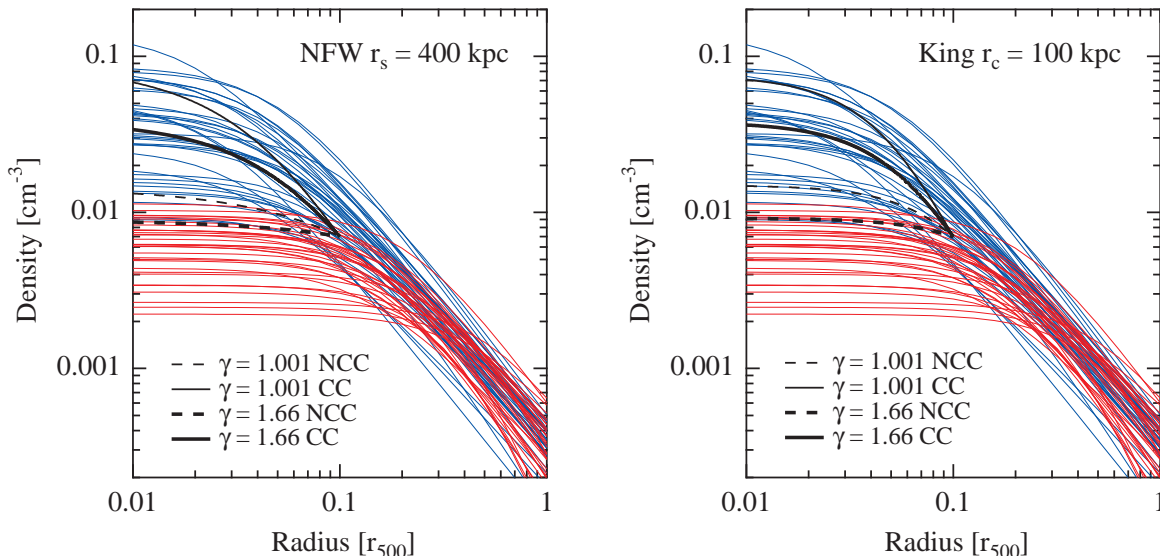


Fig. 5. Comparison of calculated gas density profiles with observations. The solid and broken black lines represent the density profiles of quasi-hydrostatic cool cores (CC) and the initial non-cool cores (NCC), respectively, for the NFW (left) and King (right) potential. The calculated density profiles are normalized such that the cooling time at r_{cool} is equal to 10 Gyr. The blue and red lines show the electron density profiles of clusters with small ($r_c < 100$ kpc) and large (> 100 kpc) core radii, respectively (taken from the β -model analysis in Ota et al. 2006.)

et al. (2006). Note that the systematic error of the central gas density derived under the isothermal β -model is estimated to be small (Appendix 1), which does not affect the present discussion. In figure 5, the solid (CC) and broken (NCC) black lines represent the density ρ' of the quasi-hydrostatic cool core and ρ of the initial polytropic non-cool core, respectively. These calculated density profiles are normalized such that the cooling time at r_{cool} is equal to 10 Gyr in the figure¹.

One can see that the initial density ρ (broken lines) falls around the upper bounds of the densities of the larger-core ($r_c > 100$ kpc) clusters, likely most relaxed but not yet cool-core ones. The density ρ' (solid lines) of the quasi-hydrostatic cool core, on the other hand, lies between the mid- and high-values of the densities of small-core ($r_c < 100$ kpc) clusters. We also found from literatures on spatially-resolved X-ray spectroscopy of clusters (Allen et al. 2001; Bonamente et al. 2006; Zhang et al. 2007; Zhang et al. 2008; Snowden et al. 2008) that 11 out of 13 small-core clusters plotted in figure 5 have a clear temperature decrease at the center while none of 17 large-core clusters has such a temperature drop.

The above facts may support that the density increase in the cool cores can be accounted for by quasi-hydrostatic cooling and our calculation gives a typical density of cool cores. However, there exists a large scatter and some observed clusters have central densities higher than predicted. In the context concerned here, the scatter is as-

cribed to that in the potential profile and/or the initial inflow condition and time elapsed.

3.2. Comparison with observed pressure and entropy profiles

Arnaud et al. (2010) discussed universal pressure profile for the REXCESS cluster sample, and obtained the best-fit profile (their equations 11–12) based on GNFW by Nagai et al. (2007). It is seen from figure 3 that the best-fit GNFW profile is close to the overall ($10 \lesssim r/\text{kpc} \lesssim 200$) slope of quasi-hydrostatic cooling gas of initially $\gamma = 1.001$ polytrope under the NFW potential. Compared to the GNFW, a depression in the mid-part could arise from discontinuity in ρ' and T' across r_{cool} (see §2.2). On the other hand, the difference at $\gtrsim 200$ kpc is due likely to that in the dark matter potential or r_s , or cluster gas is not simply hydrostatic otherwise. In any case of γ , it is unlikely that hydrostatic gas like initial polytrope here (NCC) can account for such a steep profile as the GNFW in the inner core.

Cavagnolo et al. (2009) derived radial entropy profiles of ICM for 239 clusters with the *Chandra* data (the ACCEPT sample) to find that most entropy profiles are well fitted by the model consisting of a power-law plus a constant $K(r) = K_0 + K_{100}(r/100 \text{ kpc})^\alpha$ (see also §2.2). They also showed that the distribution of central entropy K_0 is bimodal, which peaks at $K_0 \sim 15 \text{ keV cm}^2$ and $\sim 150 \text{ keV cm}^2$. From a comparison of the calculated entropy lies with the best-fit models for the ACCEPT sample (figure 4), we find that the model for clusters with higher central entropy ($K_0 > 50 \text{ keV cm}^2$) is close to the initial entropy profiles for $\gamma = 1.001$. As for $K_0 \leq 50 \text{ keV cm}^2$,

¹ The temperature at the cooling radius is assumed to be $kT(r_{\text{cool}}) = kT'(r_{\text{cool}}) = 5 \text{ keV}$ in the calculation of cooling time, whose dependence on kT is, however, sufficiently small that it does not affect the present discussion.

there is a reasonably good agreement with the CC cases in the central decrement, which is by about an order of magnitude lower than that of the initial NCC profiles.

Moreover, for the scaled temperature and the density, Arnaud et al. (2010) found that their deviations from the average scaled profile are anti-correlated with each other in the core, $r/R_{500} < 0.2$ (figure 3 in their paper); the anti-correlation is more clearly seen for cool core clusters. This behavior is in favor of quasi-hydrostatic cooling picture.

3.3. β -model fit to surface brightness profiles: physical basis of applying double- β model to cool core clusters

The density profile of the quasi-hydrostatic cool core can be mimicked by the β -model with a core radius smaller than that for the initial non-cool core, as demonstrated in figure 2. This suggests that a cool-core cluster can be still fitted to either of the β -model or double β -model, depending also on the available range of radius. Observationally, the double- β model is frequently used to fit the X-ray data of clusters having compact cores or cool cores (e.g., Ota & Mitsuda 2004; Santos et al. 2010). In this subsection, we examine whether X-ray surface brightness expected under quasi-hydrostatic cooling can be fitted by the conventional single-component or two-component β -models.

We calculate the surface brightness of free-free emission ($\propto \rho^2 T^{1/2}$ or $\propto \rho^2 T^{1/2}$ of cool or non-cool core). As readily seen in figure 6, that the gas core appears smaller in the quasi-hydrostatic cool core than the initial non-cool one. We performed the β -model fitting to the calculated surface brightness profiles with the form $S(r) = S_0[1 + (r/r_{\text{fit}})^2]^{-3\beta+1/2}$. The radial range of $5 < r/\text{kpc} < 400$ is used. The best-fit parameters are given in table 2. The surface brightness is enhanced by a factor of 2.4–6.5 and the core radius becomes smaller by a factor of ~ 2.5 –10 for the quasi-hydrostatic cool core in comparison with the initial non-cool core. In the lower panels of figure 6, the ratio of the calculated surface brightness profiles to the best-fit β models are shown. The single-component β -model gives a reasonably good fit to the NCC case, while it leaves a systematic deviation from that of the CC case. The chi-squared value defined as $\chi^2 \equiv \sum [I(r) - S(r)]^2$ is also given in table 2. Here $I(r)$ represents the calculated surface brightness profile and \sum sums up all data points.

Next, the double- β -model, $S(r) = \sum_{i=1}^2 S_{0,i}[1 + (r/r_{\text{fit},i})^2]^{-3\beta_i+1/2}$, is applied to the CC profiles. In this fitting, the inner and outer slope parameters are tied (i.e., $\beta_1 = \beta_2$) because of a large uncertainty of the inner slope and allowed to vary within 0–2. The two core radii, $r_{\text{fit},1}$ and $r_{\text{fit},2}$ are restricted to a range of 5–400 kpc. As is seen from figure 7, the surface brightness profile of clusters under radiative cooling can be well approximated by this two-component model. In fact, the systematic deviation in the single- β model fitting is significantly reduced and the χ^2 values become smaller in this case (table 2).

The above result gives a physical basis for the use of double- β model in the analysis of X-ray surface brightness of cool core clusters. We should note that the resulting $r_{\text{fit},1}$ or $r_{\text{fit},2}$ in this analysis are not necessary equal

to the core radius assumed for the potential distribution, r_c , or that expected through the relationship, $r_c \sim 0.22r_s$ (Makino et al. 1998).

The inner component with small core size of $r_{\text{fit},1} \sim 20 - 70$ kpc (table 2) can be ascribed to radiatively cooling gas at the center. The present result will also explain the fiducial emission measure profile obtained by Arnaud et al. (2002) as well as the double-peaked core-size distribution discovered by Ota & Mitsuda (2002); Ota & Mitsuda (2004), whose peak values are $r_c = 50$ kpc and 200 kpc.²

3.4. Implication on the time scale of ICM thermal evolution

The fraction of cool core clusters will give another important clue to understand the formation of cool cores since it should reflect any timescale relevant to their evolution.

Akahori & Masai (2006) calculated the probability distribution by estimating the time during which a cluster would have a certain core size, to confirm the double-peaked nature of core radius. They suggest that the gas rapidly cools after the quasi-hydrostatic condition breaks. In other words, relaxed clusters with small core radii currently observed are more or less those in the quasi-hydrostatic cooling stage, which terminates at $\sim \tau_{\text{cool}}$. Since τ_{cool} is estimated to be smaller than the Hubble time $H_0^{-1} \sim 10$ Gyr for a typical cluster, some heating is needed to sustain the system otherwise it would be unseen in \sim Gyr after virialized. Practically, however, heating due to mergers is likely invoked in the cluster evolution, as suggested also from a point of view of radio halos (e.g., Rossetti et al. 2010). The clusters of core radii > 400 kpc in the core-size distribution are attributed possibly to mergers from their morphology; it should be noted that quasi-hydrostatic cooling is a picture for a relaxed gravitational system. Also other heating/pressure sources, e.g. by black hole activity, may work. In fact, many of so-called cooling flow clusters have central cD galaxies hosting black holes. Radio mini-halos observed from these clusters may suggest the considerable contribution of the black holes.

Utilizing the technique of the X-ray fundamental plane, Ota et al. (2006) investigated the evolution of X-ray observables for the distant cluster sample. They showed that the principle axis of the plane is parallel to the t_{cool} -axis, suggesting the cooling time is a parameter to control the core structure. They also noted that the rate of radiative energy loss is likely to be kept nearly constant for a significant duration of time even after the onset of cooling in the relaxed systems. This indicates that some steady state is attained for the gas of many small-core clusters. Those results are consistently understood within the framework

² Later, a similar distribution has been shown independently by Hudson et al. (2010) using the high-resolution *Chandra* data on a nearby flux-limited sample. Notice that the detailed statistics of the cool-core formation seems to admit of further investigation (e.g., Eckert et al. 2011 and references therein), which is, however, beyond the scope of the present paper.

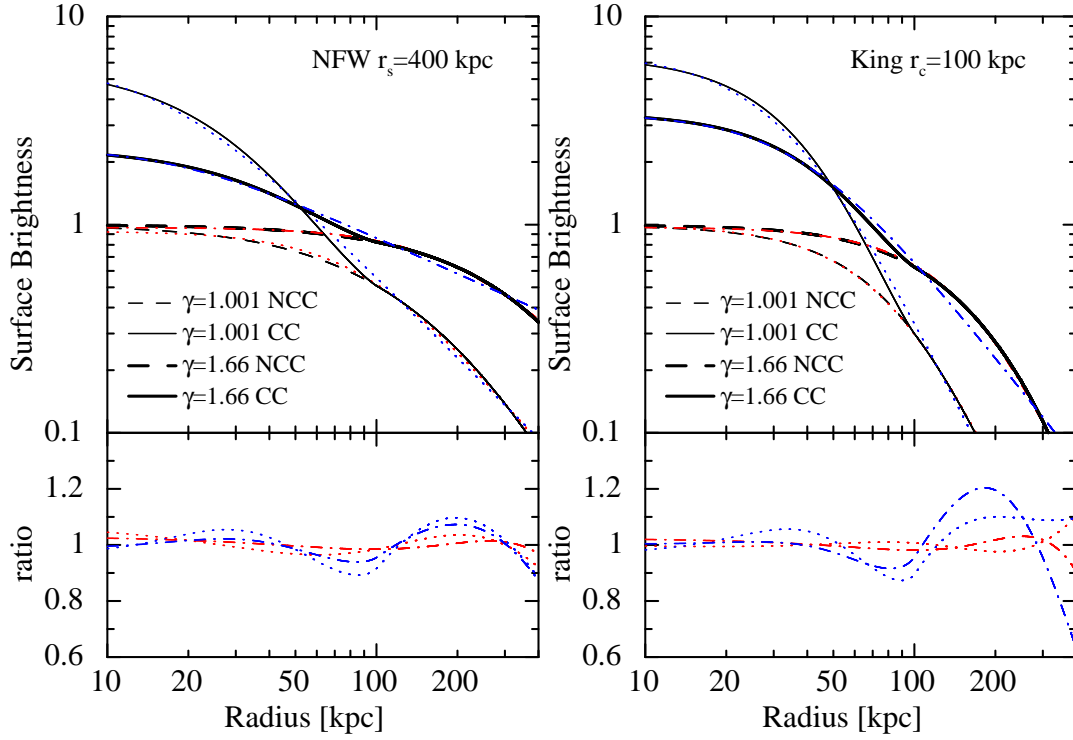


Fig. 6. Surface brightness of free-free emission calculated for quasi-hydrostatic cool cores (solid lines, CC) and the initial non-cool cores (broken lines, NCC). In the upper panels, the best-fit single β -model are also indicated with the red/blue dotted curves for the NCC/CC cases with $\gamma = 1.001$ and the red/blue dash-dotted curves for the NCC/CC cases with $\gamma = 1.66$, respectively. In the lower panels, the ratio of the calculated surface brightness profiles to the best-fit models are plotted.

Table 2. β -model parameters for surface brightness profiles in the non-cool and cool cores.

Potential	γ	Model	$S_{0,1}^*$	$r_{\text{fit},1}$ [kpc]	β_1	$S_{0,2}^*$	$r_{\text{fit},2}$ [kpc]	β_2	χ^2
NFW	1.001	NCC	single- β	0.93 (1.00)	96	0.44	—	—	1.29
NFW	1.001	CC	single- β	5.86 (5.98)	16	0.38	—	—	7.13
NFW	1.001	CC	double- β	5.14	28	0.58	0.41	237	1.61
NFW	1.66	NCC	single- β	0.97 (1.00)	191	0.37	—	—	0.41
NFW	1.66	CC	single- β	2.34 (2.36)	18	0.26	—	—	6.57
NFW	1.66	CC	double- β	1.52	38	0.57	0.78	400	0.40
King	1.001	NCC	single- β	0.99 (1.00)	93	0.69	—	—	0.10
King	1.001	CC	single- β	6.64 (6.54)	35	0.61	—	—	5.57
King	1.001	CC	double- β	6.19	51	0.94	0.23	223	0.57
King	1.66	NCC	single- β	0.97 (1.00)	190	0.75	—	—	0.49
King	1.66	CC	single- β	3.42 (3.48)	39	0.44	—	—	17.45
King	1.66	CC	double- β	2.74	74	1.19	0.69	336	0.30

* Central surface brightness normalized to that for the non-cool core. The value in parenthesis denotes the central surface brightness obtained from the present calculation.

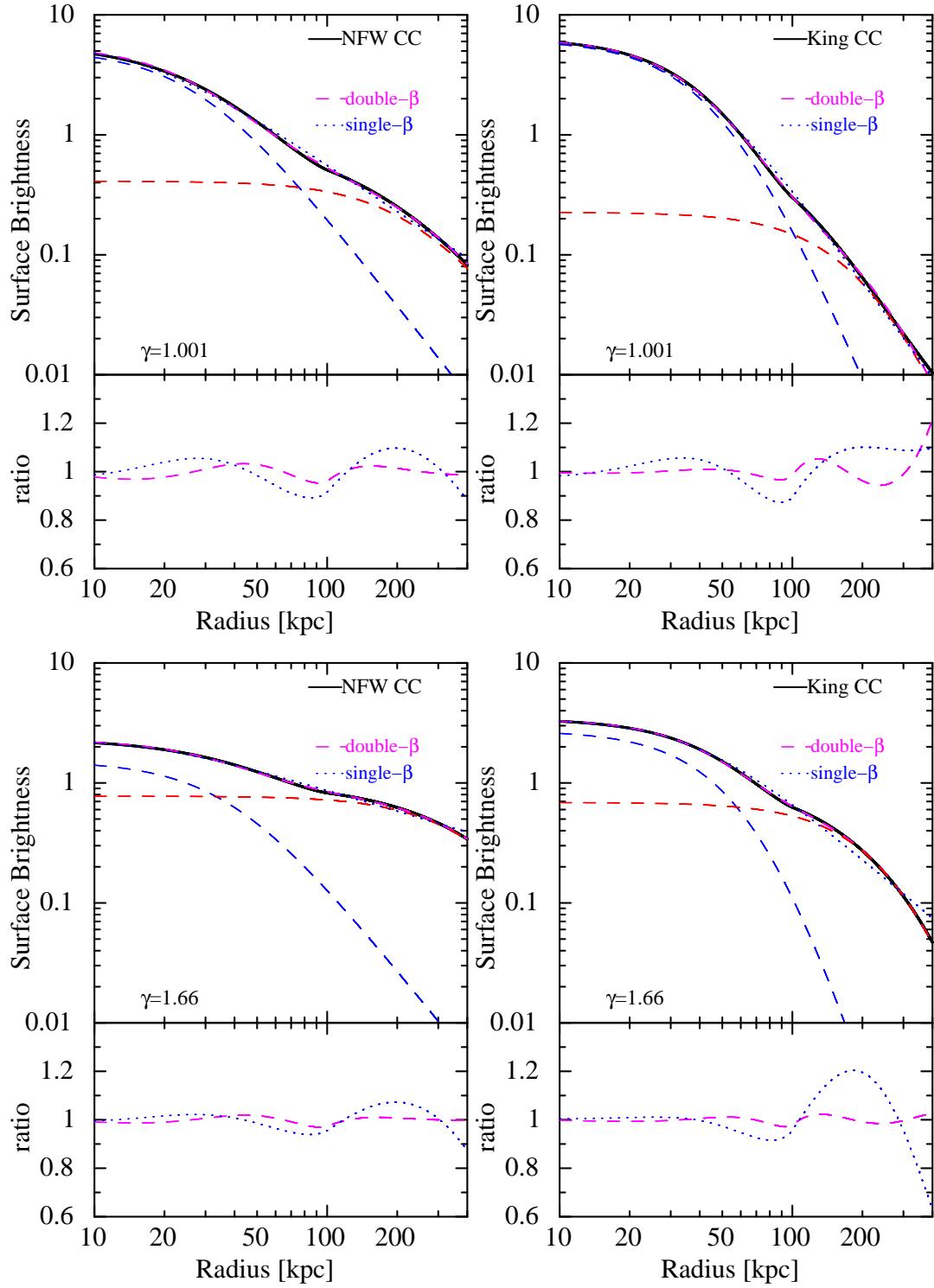


Fig. 7. Surface brightness of free-free emission calculated for quasi-hydrostatic cool cores (solid lines, CC). In the upper panels, the best-fit single- β and double- β models are indicated with the blue dotted and magenta dashed curves. The contributions of two components of the double- β model are also shown with the red and blue curves, respectively. In the lower panels, the ratios of the calculated surface brightness for the cool core to the best-fit single- β and double- β model are shown with the blue dotted and magenta dashed curves, respectively.

of quasi-hydrostatic model.

Finally, it should be noted that the present calculation shows the evolution of density profile in the cluster core when the initial NCC profile is given by $\rho(r)/\rho(0)$ in §2.1: a different initial condition may result in a different CC profile. We ignore the mass of inflow gas through our calculation. In the very late stage of quasi-hydrostatic cooling, however, the inflow gas could alter the gravitational potential in the inner core region to a steeper profile from the initial equilibrium one. This would break the quasi-hydrostatic condition and lead to the global cooling flow eventually, unless some counter pressure works against, e.g., by heating of the gas. Further investigation is needed to obtain the total view on the thermal evolution of cluster core, including the possibility of heat input due to mergers as mentioned above.

4. Summary

1. We have calculated the density profile of cool core of intracluster gas in the quasi-hydrostatic cooling phase (Masai & Kitayama 2004) assuming that the gas is initially in the virial equilibrium state within the dark matter potential represented by the NFW or King distribution and has a polytropic profile with $\gamma = 1.001$ or 1.66 .
2. In the quasi-hydrostatic cooling phase, the gas density increases by a factor of 4–6 at the cluster center while the temperature decreases to be about one-third in comparison with their initial polytropic profiles (non-cool core, NCC). Accordingly, the core radius of the cool core (CC) cluster appears more compact than the initial polytropic one. This result is consistent with the hydrodynamical simulations by Akahori & Masai (2006).
3. From the comparison with X-ray observations, it is found that the density profile of CC falls between the mid- and high-values of small-core ($r_c < 100$ kpc) when normalized so that the initial density profile has the cooling time equal to 10 Gyr at the cooling radius.
4. The pressure and entropy profiles are derived for the quasi-hydrostatic cooling gas and their CC/NCC profiles are compared with the generalized NFW pressure profile for the REXCESS cluster sample (Arnaud et al. 2010) and the best-fit entropy profile models for the ACCEPT sample (Cavagnolo et al. 2009), respectively.
5. The X-ray brightness profiles are calculated for clusters having either the NFW or King potential assuming the free-free emission. The resulting CC profiles are found to be well represented by the conventional double β -model including the central emission with a compact core size. This gives a physical basis of applying the double- β model to observed CC clusters. The inner component of the double- β model, which can be ascribed to the radiatively cooling gas at the center, will also explain the fiducial emission measure profiles (Arnaud et al. 2002)

as well as the double-peaked core-size distribution (Ota & Mitsuda 2002; Ota & Mitsuda 2004).

6. Implication on the time scale of ICM thermal evolution is discussed. Since the quasi-hydrostatic stage will terminate at $\tau_{\text{cool}} \sim \text{Gyr} < H_0^{-1}$ for a typical cluster, some heating is needed to sustain the system. The mass of inflow gas is ignored in the present calculation, however, it will alter the potential distribution of the inner core to a even steeper one in the late stage of cooling, which would break the quasi-hydrostatic balance and lead to the global cooling flow. Further investigation is needed to construct the total view on the thermal evolution, including the possibility of heat input due to mergers.

This work was supported in part by the Grant-in-Aid for Young Scientists by MEXT, No. 22740124 (NO) and by the Grant-in-Aid for Scientific Research 18540241 from JSPS (KM).

Appendix 1. Systematic error of central gas density

Ota et al. (2006) derived the electron density by the isothermal β -model fitting to the surface brightness profiles. Since the temperature dependence of X-ray surface brightness is generally small ($\propto T^{1/2}$), the systematic error of central gas density coming from the temperature drop at the cluster center is expected to be small. Actually, we made a comparison with the central gas density obtained from the *XMM-Newton* observations having improved resolutions (Zhang et al. 2007) and confirmed that there is a good agreement between the two samples as shown in figure 8. The figure includes 7 cool core clusters as well as 2 non-cool core clusters. Thus the evolution of gas density profile can be further inferred by comparing those calculated for the cool cores and non-cool ones in the present work with the β -model profiles presented in Ota et al. (2006).

References

- Akahori, T., & Masai, K. 2005, PASJ, 57, 419
 Akahori, T., & Masai, K. 2006, PASJ, 58, 521
 Allen, S. W., Schmidt, R. W., & Fabian, A. C. 2001, MNRAS, 328, L37
 Arnaud, M., Aghanim, N., & Neumann, D. M. 2002, A&A, 389, 1
 Arnaud, M., Pratt, G. W., Piffaretti, R., Böhringer, H., Croston, J. H., & Pointecouteau, E. 2010, A&A, 517, A92
 Bulbul, G. E., Hasler, N., Bonamente, M., & Joy, M. 2010, ApJ, 720, 1038
 Bonamente, M., Joy, M. K., LaRoque, S. J., et al. 2006, ApJ, 647, 25
 Cavagnolo, K. W., Donahue, M., Voit, G. M., & Sun, M. 2009, ApJS, 182, 12
 Chen, Y., Reiprich, T. H., Böhringer, H., Ikebe, Y., & Zhang, Y.-Y. 2007, A&A, 466, 805
 Eckert, D., Molendi, S., & Paltani, S. 2011, A&A, 526, A79

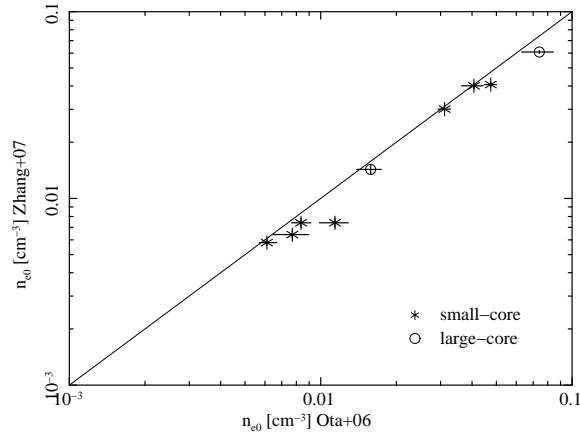


Fig. 8. Comparison of central gas density between two different samples Ota et al. (2006) and Zhang et al. (2007). The small-core and large-core clusters are denoted with the asterisks and circles, respectively

- Fabian, A. C. 1994, *ARA&A*, 32, 277
Hudson, D. S., Mittal, R., Reiprich, T. H., Nulsen, P. E. J.,
Andernach, H., & Sarazin, C. L. 2010, *A&A*, 513, A37
Jones, C., & Forman, W. 1984, *ApJ*, 276, 38
Makino, N., Sasaki, S., & Suto, Y. 1998, *ApJ*, 497, 555
Masai, K., & Kitayama, T. 2004, *A&A*, 421, 815
Nagai, D., Kravtsov, A. V., & Vikhlinin, A. 2007, *ApJ*, 668, 1
Navarro, J. F., Frenk, C. S., & White, S. D. M. 1997, *ApJ*,
490, 493
Neumann, D. M., & Arnaud, M. 1999, *A&A*, 348, 711
O'Hara, T. B., Mohr, J. J., Bialek, J. J., & Evrard, A. E. 2006,
ApJ, 639, 64
Ota, N., & Mitsuda, K. 2002, *ApJL*, 567, L23
Ota, N., & Mitsuda, K. 2004, *A&A*, 428, 757
Ota, N., Kitayama, T., Masai, K., & Mitsuda, K. 2006, *ApJ*,
640, 673
Peterson, J. R., & Fabian, A. C. 2006, *Phys. Rep.*, 427, 1
Rossetti, M., Eckert, D., Cavalleri, B. M., Molendi, S.,
Gastaldello, F. & Ghizzardi, S. 2011, *A&A*, 532, A123
Santos, J. S., Rosati, P., Tozzi, P., Böhringer, H., Ettori, S., &
Bignamini, A. 2008, *A&A*, 483, 35
Santos, J. S., Tozzi, P., Rosati, P., Böhringer, H. 2010, *A&A*,
521, A64
Snowden, S. L., Mushotzky, R. F., Kuntz, K. D., & Davis,
D. S. 2008, *A&A*, 478, 615
Suto, Y., Sasaki, S., & Makino, N. 1998, *ApJ*, 509, 544
Vikhlinin, A., Kravtsov, A., Forman, W., Jones, C.,
Markevitch, M., Murray, S. S., & Van Speybroeck, L. 2006,
ApJ, 640, 691
Zhang, Y.-Y., Finoguenov, A., Böhringer, H., et al. 2007,
A&A, 467, 437
Zhang, Y.-Y., Finoguenov, A., Böhringer, H., et al. 2008,
A&A, 482, 451